

Article

# Investigation on the Lift Force Induced by the Interceptor and Its Affecting Factors: Experimental Study with Captive Model

Rui Deng <sup>1,2</sup> , Zezhen Zhang <sup>1,2</sup>, Fuqiang Luo <sup>1,2</sup>, Pengnan Sun <sup>1,2</sup> and Tiecheng Wu <sup>1,2,\*</sup> 

<sup>1</sup> School of Ocean Engineering and Technology, Sun Yat-Sen University, Zhuhai 518000, China; dengr23@mail.sysu.edu.cn (R.D.); zhangzzh26@mail2.sysu.edu.cn (Z.Z.); luofq5@mail2.sysu.edu.cn (F.L.); sunpn@mail.sysu.edu.cn (P.S.)

<sup>2</sup> Southern Marine Science and Engineering Guangdong Laboratory (Zhuhai), Zhuhai 519082, China

\* Correspondence: wutch7@mail.sysu.edu.cn; Tel.: +86-187-4514-7797

**Abstract:** An interceptor is an appendage widely used for high-speed planing boats to reduce resistance and modify hull attitude by the lift force-induced, but the relationship between the induced lift force and the factors affecting it are still not clear, especially for the vessels other than the planing hull. In this paper, a model test of a series of models is performed to investigate the lift force induced by an interceptor and the influence of the affecting factors systematically. The lift forces induced by the interceptor are tested in the conditions of different velocities, interceptor heights, angles, and drafts in the towing tank. The effects of each factor and the coupled effects are analyzed. It is found by the experimental results that the lift coefficient of the induce lift force in the present investigation is approximately proportional to the square of the non-dimensional velocity and interceptor height, but the effect of the interceptor height is of a limited extent. The influence of angle and draft on the lift force induced by the interceptor cannot be ignored in the present study. The induced lift force is decreased when the angle of the plate is reduced and is enhanced when the draft is increased.

**Keywords:** interceptor; lift force; velocity; angle; draft



**Citation:** Deng, R.; Zhang, Z.; Luo, F.; Sun, P.; Wu, T. Investigation on the Lift Force Induced by the Interceptor and Its Affecting Factors:

Experimental Study with Captive Model. *J. Mar. Sci. Eng.* **2022**, *10*, 211. <https://doi.org/10.3390/jmse10020211>

Academic Editor: Kostas Belibassakis

Received: 16 January 2022

Accepted: 2 February 2022

Published: 5 February 2022

**Publisher's Note:** MDPI stays neutral with regard to jurisdictional claims in published maps and institutional affiliations.



**Copyright:** © 2022 by the authors. Licensee MDPI, Basel, Switzerland. This article is an open access article distributed under the terms and conditions of the Creative Commons Attribution (CC BY) license (<https://creativecommons.org/licenses/by/4.0/>).

## 1. Introduction

A small structure that is perpendicular to the flow direction is considered a powerful appendage modifying the flow field, such as the wing flap of the plane and the interceptor of the ship. An interceptor is a thin plate mounted on the stern and generally perpendicular to the water line, which is recommended to improve the hydrodynamic performance and navigation attitude easily, economically, and in an environmentally friendly way. There are also some additional functions of the interceptor. Zeselezcky et al. [1,2] proposed that an interceptor plays an important role in increasing lift force, decreasing resistance, and improving the propulsion efficiency of warships. Interceptors have also been widely used in recent years for high-speed crafts in ride and trim control [3]. Karimi et al. [4] demonstrated that the heave, pitch motion, and vertical acceleration can be reduced by an interceptor through model tests on the performance of high-speed catamaran planing boats in calm water and waves. As pointed out by Park et al. [5], the pitch motion is reduced by up to 41.3% in the regular wave and 32.4% in the irregular wave by a controllable interceptor system. Even the porpoising motion of high-speed crafts can be mitigated obviously by the interceptor [6]. In addition, interceptors can be used to harness hydro-energy at the wash of fast boats [7].

Due to the outstanding advantages of the interceptor, there have been many studies of it since its function was found by researchers and more and more attention is paid to exploring the mechanism of the influence. Ghassemi et al. [8] conducted a model test on a yacht with the interceptor, finding that high pressure is induced in the region between the interceptor and the bottom, and the wetted surface and resistance is reduced by the interceptor. In 2017, Mansoori et al. [9–11] investigated the flow field around the

interceptor in the conditions of different heights by model tests and CFD and found that a remarkable pressure gradient is induced by the interceptor and the resistance of the hull is therefore reduced. The investigation of Guo et al. [12] demonstrated that the wake flow and navigation attitude of the hull is changed by the interceptor, and the wave resistance and the wetted surface, as well as the frictional resistance, is reduced. In the study of Zhu et al. [13], it is indicated that the splashing resistance on both sides of the hull and the residual resistance were reduced for the improved pressure distribution, and navigation attitude and virtual length were modified by the interceptor, which is consistent with the conclusions obtained by Song et al. [14]. The investigation on the planing boat performed by Shen et al. [15] indicated that the trim angle is reduced because of the variation of the pressure distribution caused by the interceptor. Then, Seok et al. [16] conducted research on the effect of the interceptor on the pressure distribution. By the experiment of the high-speed displacement ship conducted in the towing tank, Pacuraru et al. [17] found that the resistance can be reduced by up to 14% by the interceptor in the condition of high Froude numbers. In addition, in order to analyze the effect caused by the interceptor, new technologies have been applied to discover the details of the flow field. Pressure reconstruction technology using three-dimensional scanning PIV is adopted in Jacobi's research [18], which is based on the time-averaged velocity field measurement in the experiment. The effect of the interceptor's height on the pressure distribution at the center plane of the model is discussed. Song et al. [19] used SPIV and RANS to investigate the influence of the interceptor on the inlet velocity distribution of water-jet propulsion. It is shown by the results that the resistance and the momentum are reduced by 6.06% and 2.1% on average.

The efficiency of the interceptor is influenced by many factors, including those of the interceptor and the hull. The height of the interceptor is an important factor as pointed out by Ghassemi et al. [8], and it has a close relationship with speed. This conclusion is confirmed by Mansoori et al. [9–11]; however, in Mansoori's investigation, the length of the hull and the thickness of the boundary layer should be taken into account. To get a better design of the interceptor for the trim optimization and minimum resistance of the planing boat, Mansoori et al. investigated the major geometric parameters (height and width) of interceptors. The same conclusions are obtained by Shen et al. [15], namely, that an appropriate height of the interceptor is helpful in obviously reducing the resistance of the planing boat and increasing motion stability. Seok et al. [16] performed a detailed investigation. In their study, it is found that the pressure on the bottom of the hull is increased in proportion to the speed and the height of the interceptor for the blocking effect of the interceptor. Suneela et al. [20] considered that the height of the interceptor plays an important role in the vessel's performance. The location of the interceptor is also one of the important factors. It is pointed out by the model test performed by Karimi et al. [3] that ship resistance and motion is obviously reduced by an interceptor that is located at the stern and midship, and the maximum drag reduction for a mono-hull vessel and catamaran reaches 15% and 12%, respectively. The related studies [21] on the influence of hull parameters are very limited. It is indicated by Sverre [22] that the effect of the draft and deadrise angles on the resistance and lift force of the traditional planing boat with an interceptor is negligible. Based on that conclusion, an approximate formula is given to estimate the induced lift of the interceptor for the first time. However, it is a function of hull breadth and interceptor height, which ignores speed and other hull factors. Moreover, Steen's conclusion is aimed at the planing boat in the condition of free motion. The lift force induced by the interceptor cannot be obtained exactly for the changing attitude of the hull. Meanwhile, it is unknown whether this formula is suitable for the other types of ships. Srikanth et al. [23] conducted a model test of a prismatic planing boat with a deadrise angle of  $20^\circ$  considering the effect of different interceptor heights, draft, and the center of gravity. Finally, a dimensionless equation of the longitudinal moment was concluded by the results of the model test and the SIT method [24] to evaluate the performance of planing boat in the conditions with or without the interceptor. It is demonstrated by the experimental results that the resistance

of the model cannot be reduced by the interceptor, even in the condition of high speed. Luca et al. [25] derived a new conclusion by the investigation that the resistance reduction caused by the interceptor has a close relationship with the deadrise angle, which is different from the one obtained by Sverre [22].

It can be found in the literature review that the principle of the effect caused by the interceptor on planing boats is caused by the high pressure induced by the interceptor. However, although the mechanism is unveiled by the previous achievements, the application of the interceptor on the other types of vessels is still needed to be investigated. The investigation performed by Mansoori et al. [26] is constructive because a general rule of the effect caused by the interceptor was obtained by adopting a 2-D flat plate rather than a specific hull form. Both numerical simulation and model tests were conducted to study the flow field around the plate with the interceptor, then the flow field details were given to estimate the lift force induced by the interceptor. In the study, the plate was perpendicular to the free surface, which was easy to conduct and observe. However, a problem is also caused by this approach, namely, the flow field is changed with draft and influenced by the wave generated on the free surface.

It is shown in the literature survey that the lift force induced by the interceptor is known as the reason for resistance reduction and hull attitude optimization for planing boats. Meanwhile, the relationship between the induced lift force and some factors remains unknown even for planing boats. The relationships that take the influence of the hull form into account are important for the design of the interceptor. A well-designed interceptor is good at improving the speed and attitude of the hull. Compared to the planing boat, mon-hull high-speed vessels are much more thirsty for the well-designed interceptor. In this paper, considering the research gap of the above investigation, three modified models are designed for the model test to investigate the effect of the interceptor. These models consist of plates with different angles and waterproof plates which are perpendicular to the free surface. The flow field around the plates with the interceptor is not influenced by the waves on the free surface because they are submerged deep from the free surface, and no lift force is induced by the waterproof plate for it is perpendicular to the free surface. Systematic model tests are carried out in the present study investigating the lift force induced by the interceptor and the factors that influence it. The effect of the factors, such as the height of the interceptor, speed, angle of the plate, draft, and the coupled effects of them are analyzed in detail. The results of the experiments performed will provide support to the physics of the lift force induced by the interceptor as well as provide experimental data for the validation of numerical models. This paper is organized as follows: In Sections 2 and 3, the test model and experimental setup are described in detail. Section 4 presents the results and analysis of the effect of the factors. In Section 4.1, the velocity, as the primary factor affecting the lift induced by the interceptor, is analyzed firstly, and the influence of velocity on the lift force induced by the interceptor and the change rate of lift force under the same height of the interceptor is studied. In Section 4.2, the interceptor heights affecting the lift force are further studied in two different perspectives under the same velocity. In Section 4.3 and 4.4, the difference of different angles and drafts affecting the lift force induced by the interceptor is analyzed in two ways, respectively. With the increase of angle or draft, lift coefficients show a decreasing trend but show a contrary trend on the change rate of lift coefficients. So, the coupling effects of the angle and draft are studied. Section 5 provides a summary of this study.

## 2. Test Model

In this study, in order to investigate the general relationship between the lift force induced by the interceptor and some factors, three plates (including a flat plate and two V-type plates) are adopted. To eliminate the influence of the free surface, the plates are located underwater. The waterproof plate which is perpendicular to the free surface is connected to the plate at its edge to keep the devices away from water. Besides, the entrance of the test model is geometrically smoothed in order to mitigate the disturbance on the

free surface, which makes the models look like ships. The length of the models on the free surface is 3.0 m, which will minimize the influence of the entrance on the interceptor. The parameters of models, the height of the interceptor, the draft, and the velocity adopted in the test are shown in Table 1. The three models are shown in Figure 1. The 3D view of the test models is demonstrated in Figure 1a, and the lines plan is shown in Figure 1b. The detailed design of the interceptors is shown in Figure 1c, and the location of the interceptors is demonstrated in Figure 1d.

**Table 1.** Main parameters of the testing model and conditions.

Model	L (m)	B (m)	$\alpha$ (°)	h (mm)	T (cm)	V (m/s)
1	3.0	0.375	180	0, 7.0, 10.0, 15.0	5.0	1.0, 1.5, 2.0, 2.5, 3.0
2	3.0	0.375	160	0, 7.0, 10.0, 15.0	5.0, 10.0	1.0, 1.5, 2.0, 2.5, 3.0
3	3.0	0.375	140	0, 7.0, 10.0, 15.0	10.0	1.0, 1.5, 2.0, 2.5, 3.0

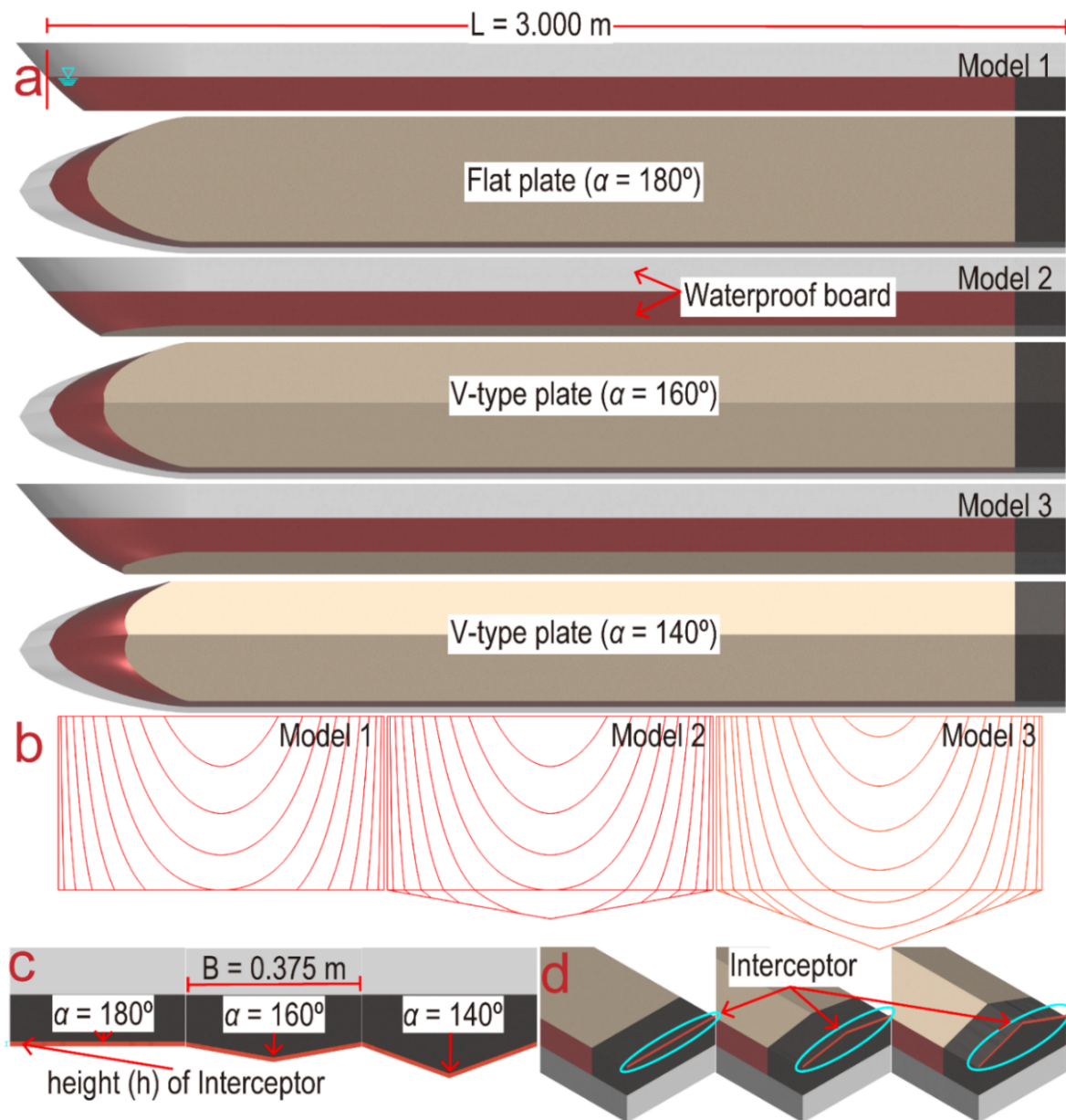


**Figure 1.** Test models: (a) 3D view, (b) Lines plan, (c) Detailed design of the interceptors, and (d) Location of the interceptors.

Where  $\alpha$  is the angle of the V-type plate,  $h$  is the height of the interceptor, and  $T$  is draft. It is important to note that when the angle of the V-type plate is  $180^\circ$ , it is a flat plate. Draft  $T$  is defined as the vertical distance between the side edge of the bottom and the free surface, which is 5.0 and 10.0 cm in the present study. The interceptor is fixed at the end of the bottom, the width of which is inconsistent with the model's width, extending outwardly and perpendicular to the free surface. The distance that the interceptor extends from the plate is defined as the height of the interceptor  $h$ . Considering the previous investigation performed by the researchers mentioned above, especially Mansoori, the heights of the interceptor used in the present test are 7.0, 10.0, and 15.0 mm, and the ratio of the interceptor height to the beam is about 1.9%, 2.7%, and 4.0%, respectively. The experiments of the models mentioned above are carried out, and the relationship between the lift force induced by the interceptor and the factors are investigated, as well as the coupling effects of angle and draft.

### 3. Experimental Setup

#### 3.1. Facility

The experiment was conducted in the towing tank of Harbin Engineering University. The length, width, and depth of the towing tank are  $108 \text{ m} \times 7 \text{ m} \times 3.5 \text{ m}$ . The carriage is controlled by a microcomputer, the stable range of the towing speed is 0.100–6.500 m/s, and the speeds adopted in the present test are 1.0, 1.5, 2.0, 2.5, and 3.0 m/s, the  $Fr$  numbers of which are about 0.184, 0.277, 0.369, 0.461, and 0.553, respectively. The force transducer used in this test is a three-component sensor. The scales used in the longitudinal, transverse, and vertical ranges are 60 kg, 60 kg, and 120 kg, respectively. The corresponding measurement accuracy is not greater than 0.1% full scale, and the 16-channel data acquisition device was used for data collection. The collection frequency is 40 Hz.

#### 3.2. Lift Force Induced Experimental Measurement Scheme

Karimi et al. [4] found that the reason that the hull resistance could be reduced by the interceptor was the lift force induced by it. When the lift force is induced, the hull rises, and the wetted surface is reduced. Meanwhile, the wake flow is optimized, and the hull attitude is changed by the lift force. This point of view is accepted by all the researchers and the mechanism is illustrated in Figure 2.

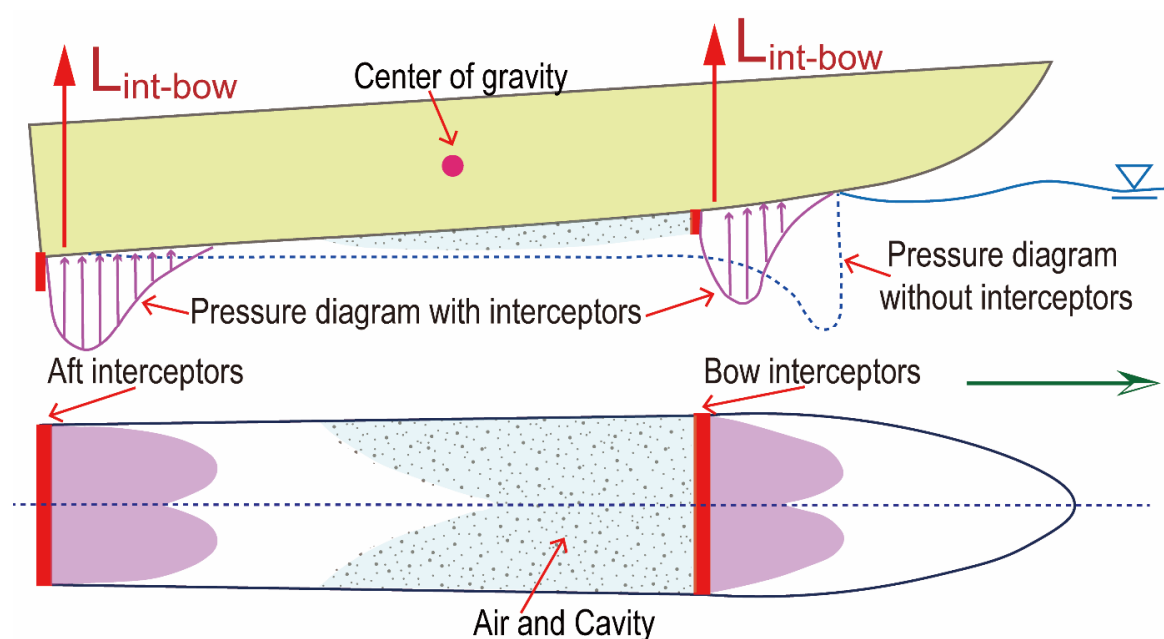
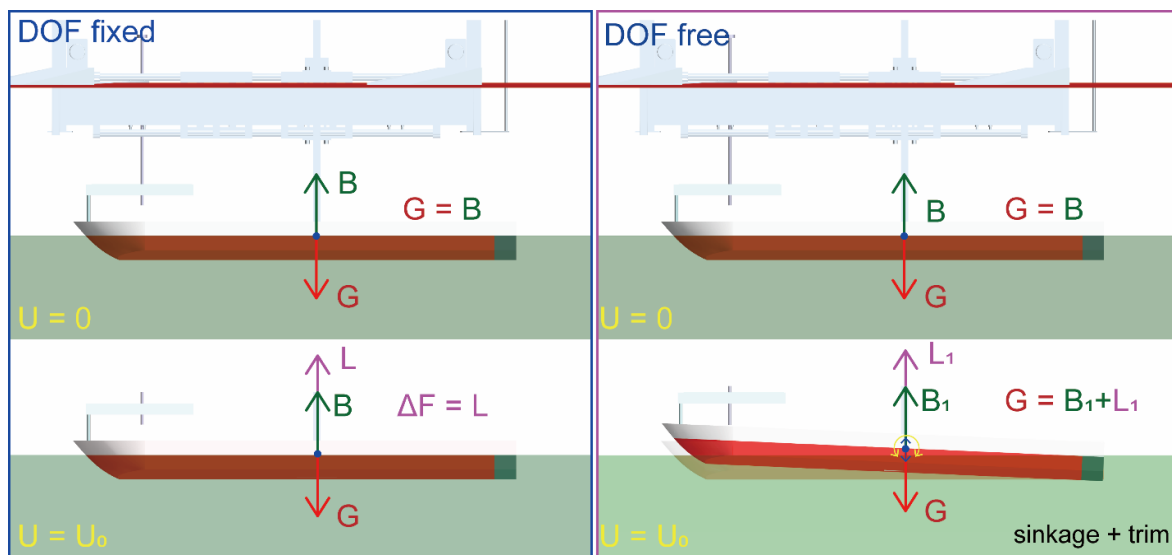


Figure 2. Illustration of physical phenomena and mechanisms associated with interceptors.

It is indicated that if the lift force induced in each condition can be obtained and the variation of the wetted surface and trimming moment can be estimated, then the resistance and the trim could be calculated primarily. Therefore, the root of the problem is the induced lift force. An illustration of the method is shown in Figure 3. In order to obtain the rules between the induced lift force and the factors affecting it, the Dof fixed model test must be adopted. When the velocity of the test model with the interceptor is  $U = U_0$ , the gravity  $G$  is not changed, the buoyancy  $B$  is not varied for the displacement or change in the condition of the captive model test, and the variation of the resultant force in the vertical direction  $\Delta F$  is the force induced by interceptor  $L$  under the Dof fixed test scheme. If the model test is performed by a Dof free model when the sinkage or trim is changed, the lift force induce is balanced by the gravity, and the gravity  $G$  equals the sum of the lift force  $L_1$  and buoyancy  $B_1$  ( $G = B_1 + L_1$ ). The gravity of the model is not changed whether in the captive model test or free model test, so the resultant force in the vertical direction is 0 in the Dof-free model test. It can be found in the literature review that almost all the experiments investigating the influence of interceptors were conducted in the condition of free motion in trimming and sinkage. The advantage of this approach is that the effect caused by the interceptor on hull attitude and resistance can be obtained directly. However, for the investigation of the lift force in the present study, this approach is not acceptable because the induced force will be mitigated by the variation of the hull attitude. In addition, there is a remarkable difference in the hull attitude between the conditions of static and sailing. It is unreasonable to consider the impact of the interceptor as a function of the initial state. Considering the problems above, a series of 6-DOF restrained model tests are adopted in the present study. The vertical resultant force in the condition of static, which includes the buoyancy and weight of the model, is obtained before each test. The vertical resultant force in the condition of sailing, which includes buoyancy, the weight of the model, and the hydrodynamic force induced by the interceptor, is obtained again in the test correspondingly. Therefore, the difference between them is the lift force induced by the interceptor in the corresponding condition.



**Figure 3.** Experimental scheme of Lift force obtained by Dof fixed (Left) and Dof free (Right) model.

### 3.3. Detailed Setup of Towing Tank Test

The experimental setup is described in detail as follows: The front view of the experimental setup in the towing tank is demonstrated in Figure 4a, and the side view of the experimental setup in the towing tank is shown in Figure 4b. The close-up of the schematic diagram is demonstrated in Figure 4c, and the photograph of towing test carried out is shown in Figure 4d. The force transducer is shown in Figure 4e, and the wake flow caused

by the interceptor is demonstrated in Figure 4f. In the experiment, the model is connected to the force transducer directly, which is fixed at the intersection of the longitudinal section, the middle section, and the free surface. The force transducer is connected to the carriage by a center post. Guidance is used to restrain the yaw and sway motion of the model.

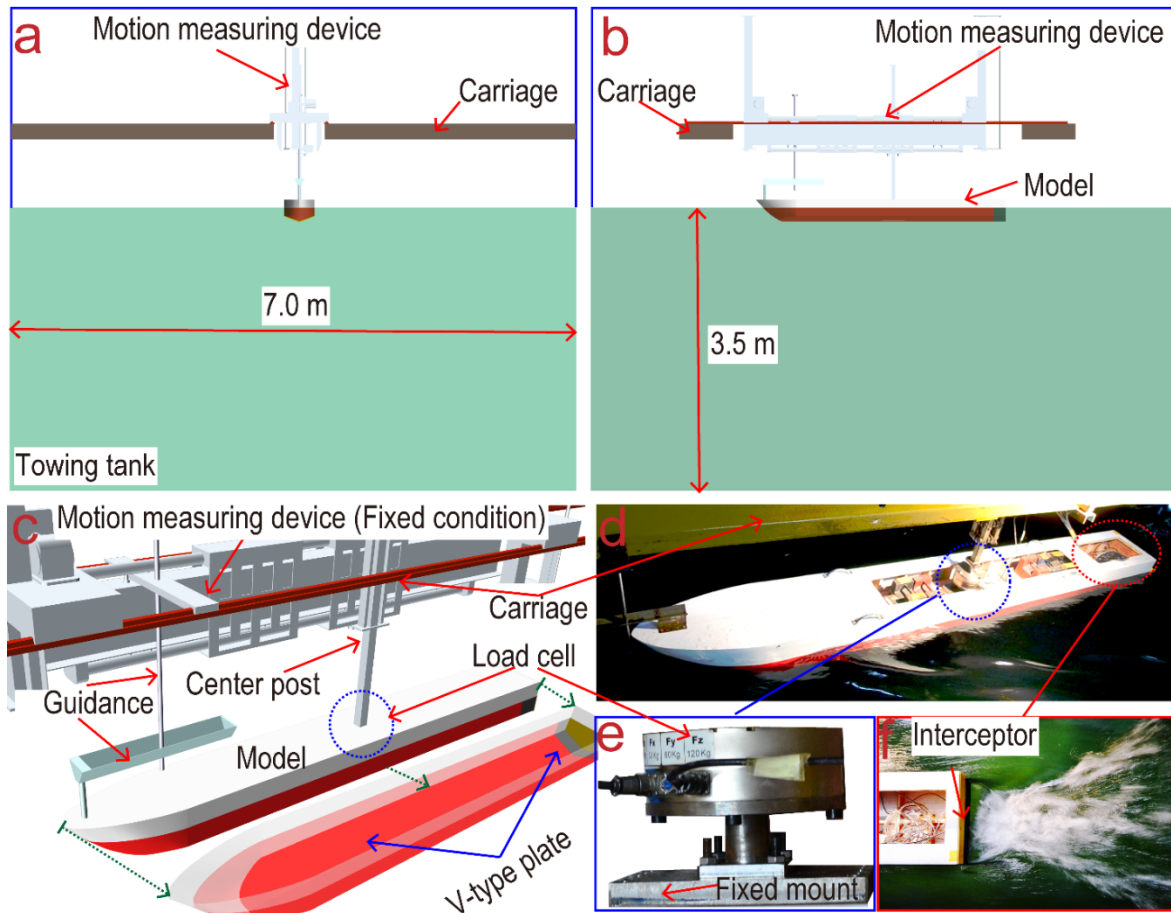


**Figure 4.** Experimental setup: (a) Front view of the experimental setup in the towing tank, (b) side view of the experimental setup in the towing tank, (c) Close-up of schematic diagram of the experimental setup, (d) Photograph of the test model in the towing tank, (e) Force transducer, and (f) Wake after the stern with the interceptor.

The scheme used in the present model test to analyze the effect of the interceptor and the influence of the factors on the effect of the interceptor is shown in Figure 5. Model 1, the angle of which is  $180^\circ$ , is tested in the conditions of 5.0 cm draft and different interceptors, at first, in order to obtain the basic law of the effect caused by the velocity and the height of the interceptor. Then, Model 2, which is formed by reducing the angle to  $160^\circ$  while keeping the constant draft of Model 1, is tested. The effect of the angle can be obtained by comparing the results of Model 1 and Model 2 in the condition of the constant draft. After that, the model test is performed in the condition that the draft of Model 2 is increased while keeping it at a constant angle. The effect of the draft can be obtained by the comparison of the test data of Model 2 in different drafts. Lastly, Model 3 is formed by reducing the angle of Model 2 from  $160^\circ$  to  $140^\circ$ . The coupling effect of the angle and draft is obtained by the comparison of the test data of Model 1 and Model 2 in different drafts, Model 2 and Model 3 in different drafts, as well as Model 1 and Model 3 in different drafts. Photographs of phenomena under typical working conditions are shown in Figure 6. The velocity of the ship and the height of the interceptor usually have a direct effect on the virtual length of the ship and the range of the rooster tail. It can be seen from Figure 6 that, as the speed increases, the virtual length of the stern increases, and the spread angle of the rooster tail on the

horizontal plane decreases. As the height of the interceptor increases, the virtual length of the ship increases, and the spread angle of the rooster tail in the horizontal plane decreases, and under the same conditions, it is more pronounced under high-speed conditions.

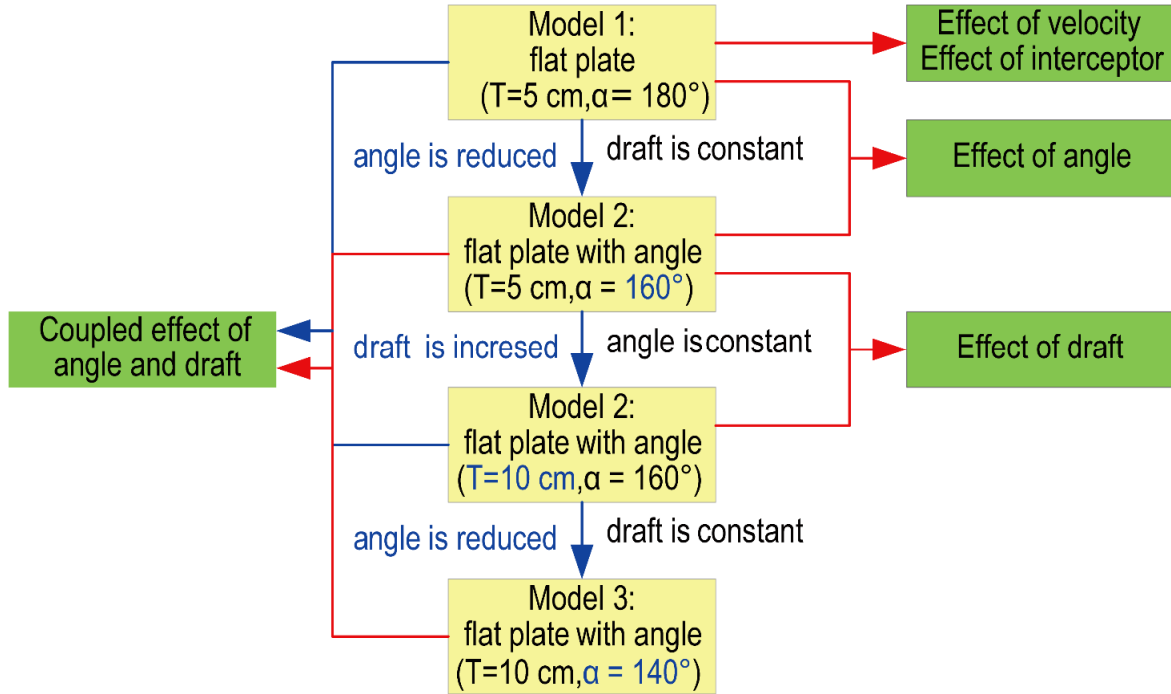


Figure 5. The scheme adopted in the investigation.

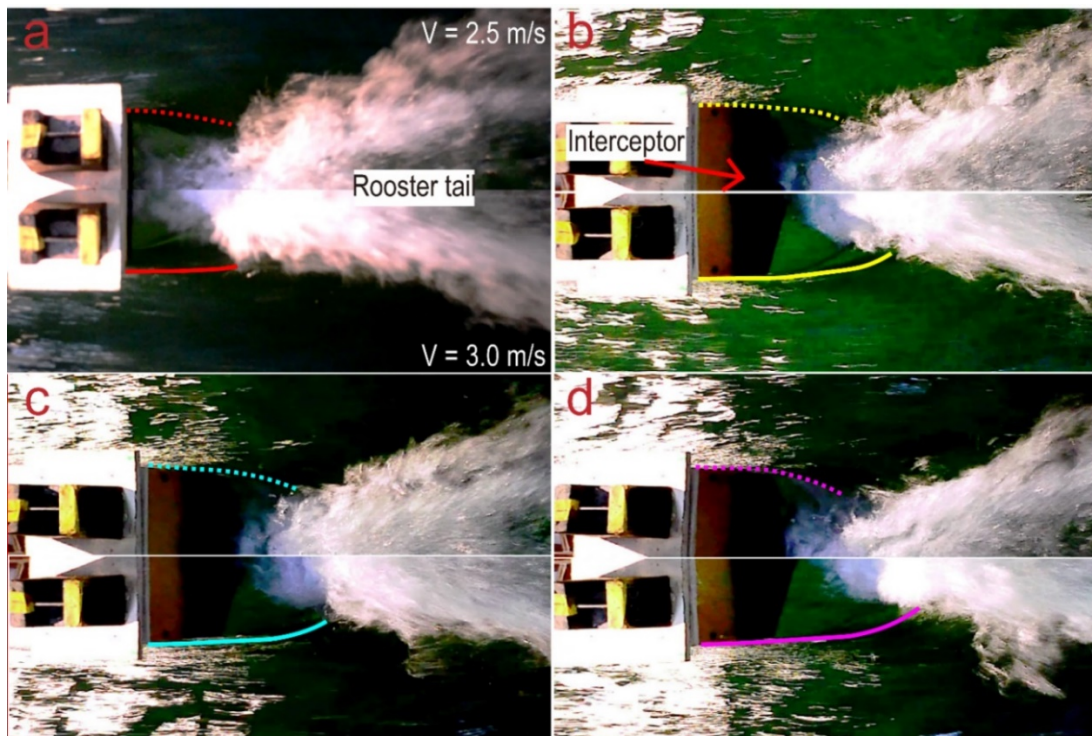


Figure 6. Photographs of phenomena under typical working conditions: (a)  $\alpha = 160^\circ$ ,  $T = 10.0\text{ cm}$ ,  $h = 0$ , (b)  $\alpha = 160^\circ$ ,  $T = 10.0\text{ cm}$ ,  $h = 1.9\% B$ , (c)  $\alpha = 160^\circ$ ,  $T = 10.0\text{ cm}$ ,  $h = 2.7\% B$ , and (d)  $\alpha = 160^\circ$ ,  $T = 10.0\text{ cm}$ ,  $h = 4.0\% B$ .

### 3.4. The Main Sources of Uncertainty in the Towing Tank Test

A detailed analysis of the uncertainty of the towing tank test is a professional research topic. The focus of this article is to study the lift force induced by the interceptor and its influencing factors. It is difficult to add a very detailed test uncertainty analysis in the limited space of this article. In order to show the experimental setup and results more rigorously, the main sources of uncertainty in the towing tank test are described accordingly:

- (1) The error of the towing tank equipment condition: The stability and accuracy of the speed of the towing carriage in the towing tank is a very important factor. The maximum speed of the towing carriage is 6.5 m/s, and its global speed control tolerance is within 0.3% in this study;
- (2) The error of the ship model design and processing: The ship models used in this study are made of glass fiber reinforced plastic, and the surface of the hull is clean and smooth. When the model processing is completed, the processing accuracy of the model is checked using the model inspection platform. The error of the model length is less than 1.0 mm, and the error of half-width below the design waterline is less than 0.5mm, which meets the relevant requirements;
- (3) The error of the setup of the towing test of the lift force induced by the interceptor:
  - (a) For model connection and installation: The ship model is connected with the center post of the motion measuring device through a connecting flange. After the model is connected, a line laser will be used for collimation correction, so the longitudinal centerline of the motion measuring device is in the same vertical plane as the centerline of the ship model. The error caused by the connection and installation is very small and can be ignored;
  - (b) For the measurement system: The induced lift measurement system is calibrated before this experiment. Furthermore, the calibration is performed by using a standard weight as the assumed lift force induced by the interceptor and recording the output value of the force sensor. The force transducer used in this test is a three-component sensor, the scales used in the longitudinal, transverse, and vertical ranges of 60 kg, 60 kg, and 120 kg, respectively, the corresponding measurement accuracy is not greater than 0.1% full scale;
  - (c) For the measured external environment: the change of water temperature in the towing tank directly affects the viscous force and Reynolds number of the ship model. Our test is completed in the same time period, and the temperature is collected multiple times during the test every day. The temperature difference of the test under different working conditions is within 0.1 degrees;
- (4) The error of the test result analysis and conversion method: The measurement results in this article are comparatively analyzed at the model scale, without real-scale extrapolation based on any assumptions. The data under different working conditions use the same conversion method, so the error in this part can be ignored.

In addition, for the uncertainty of the towing test of the towing tank in Harbin Engineering University, Zhou [27] had carried out a very detailed uncertainty analysis, and the results of the towing tank in Harbin Engineering University are also compared with the report of China Ship Scientific Research Centre (CSSRC), Marine Design and Research Institute of China (MARIC), and Shanghai Ship and Shipping Research Institute (SSRI), and the measurement results agree well.

## 4. Results and Analysis on the Effect of Factors

It is indicated by the investigation performed by Mansoori et al. that the lift force induced by the interceptor is the primary reason for resistance reduction, so a series of model tests are used to investigate the variation of lift force in different conditions, ignoring the resistance. The effects of the interceptor, velocity, angle, draft, as well as the coupling effect of angle and draft, are analyzed based on the test data. Because the experimental conditions are limited and the details of the flow field, such as the pressure distribution on the plate and vortex shedding cannot be obtained in the test, more details can be found in the previous investigations based on CFD [28].

#### 4.1. Effect of Velocity

Velocity is considered the primary factor affecting the lift induced by the interceptor. The speeds adopted in the model test are 1.0, 1.5, 2.0, 2.5, and 3.0 m/s, namely,  $Fr = 0.184, 0.277, 0.369, 0.461,$  and  $0.553$ . Where  $Fr = V/\sqrt{gL}$ ,  $V$  is the test velocity,  $g$  is the gravitational acceleration, and  $L$  is the longitudinal length of the plate. The heights of the interceptor  $h$  are 0, 7.0, 10.0, and 15.0 mm, which are about 0, 1.9%, 2.7%, and 4.0%  $B$ , where  $B$  is the width of the plate.

The coefficient of the lift force is calculated by Equation (1), and the coefficients of lift force in different conditions are compared in Figure 5.

$$Cl = \frac{L}{0.5\rho V^2 S} \times 10^3 \tag{1}$$

where  $Cl$  is the lift coefficient,  $L$  is the lift force obtained in the corresponding condition, which is the resultant force of buoyancy, the weight of the model, and hydrodynamic force in the vertical direction. The lift force  $F_l$  is 0 when the speed of the model equals 0.  $\rho$  is the fluid density,  $V$  is the speed of the model, and  $S$  is the projected area of the plates on the free surface, which is about  $1.068 \text{ m}^2$  for the three models.

As it is shown in Figure 7, the coefficient of the lift force is negative because the resultant force of buoyancy, weight of the model, and hydrodynamic force in the vertical direction are 0 in the condition that the speed of the model equals 0, and the pressure acting on the plate is decreased based on the Bernoulli equation when the speed is larger than 0 and the attitude of the model is restrained, which means the resultant force of buoyancy and hydrodynamic force is less than the weight of the model. It is shown in Figure 5, that, for the plates with different interceptor heights, when the  $Fr$  is less than about 0.277, the coefficient of the lift force is decreased with the velocity. When the  $Fr$  is larger than about 0.277, the coefficient of the lift force is increased with the velocity in a positive correlation and the same tendency at different interceptor heights. The transition of the curves is caused by the change of dominant position of bottom pressure, namely transforming from static pressure to hydrodynamic pressure. Besides this, all curves exhibit the same trend, so it is reasonable to consider that  $Fr \approx 0.277$  is a turning point of bottom pressure. It is indicated by the results that velocity is a key factor dominating the coefficient of lift force. The lift coefficient is changed with the velocity in the same way for the plates with different interceptor heights. Taking the results in the entire velocity extent adopted in the model test into account, the lift coefficient is proportional to the square of  $Fr$ , approximately.

In order to analyze the variation of the lift at each velocity, a factor  $R_v$  is defined as follow:

$$R_{v(i)} = \frac{Cl_{v(i+1)} - Cl_{v(i)}}{|Cl_{v(i)}|} \tag{2}$$

where  $Cl_{v(i)}$  is the lift coefficient of the current speed,  $Cl_{v(i+1)}$  is the lift coefficient of the next speed, and the factor  $R_v$  indicates the change rate of lift coefficient caused by velocity. The  $Fr$  adopted are 0.184, 0.277, 0.369, and 0.461, and the factor  $R_v$  in different conditions are compared in Figure 6.

It is shown in Figure 8 that there is a nonlinear relationship between the change rate of lift coefficient and non-dimensional velocity, the lift coefficient is increased with the velocity when the  $Fr > 0.184$ , and the change rates are varied from speed to speed, which means the contribution of velocity is nonlinear. The change rates in the conditions of different interceptors possess the same tendency and little difference, which suggests that the influence of velocity is greater than that of the interceptor. Further, the change rate is affected by the interceptor at each velocity, and the influence is proportional to the height of the interceptor, but there is a limited extent of the interceptor height beyond which has little affection. Further discussion will be conducted in Section 4.2.

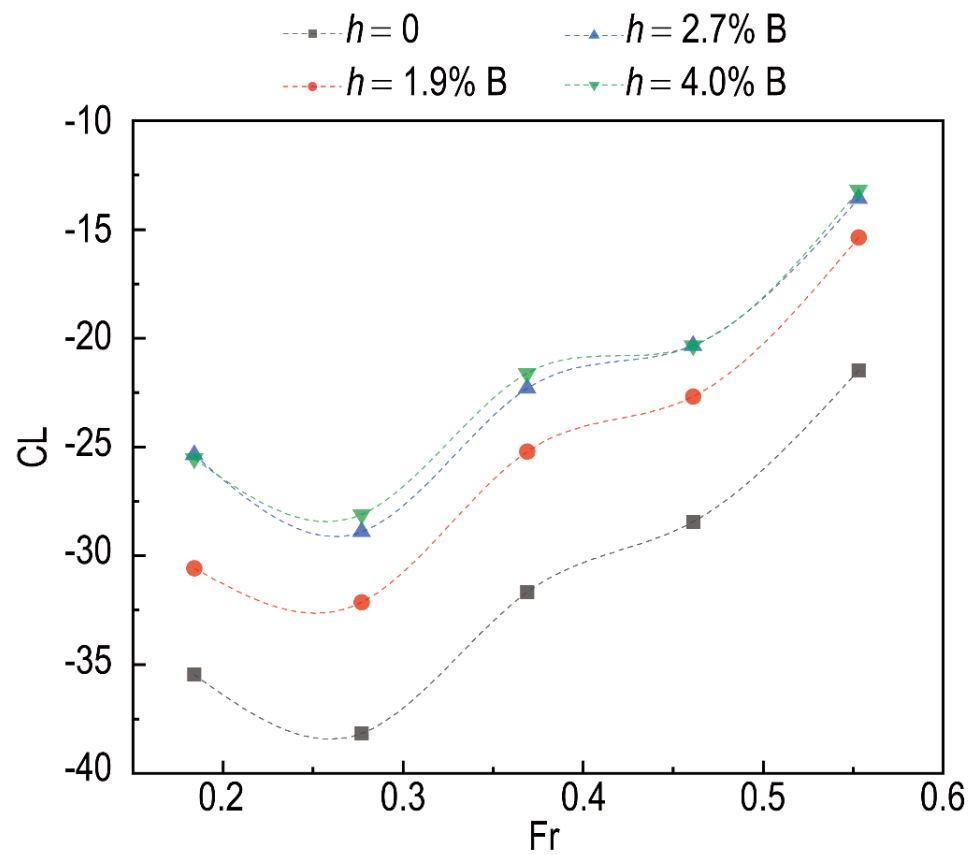


Figure 7. Comparison of the lift coefficients in the conditions of different velocities ( $\alpha = 180^\circ$ ,  $T = 5.0$  cm).

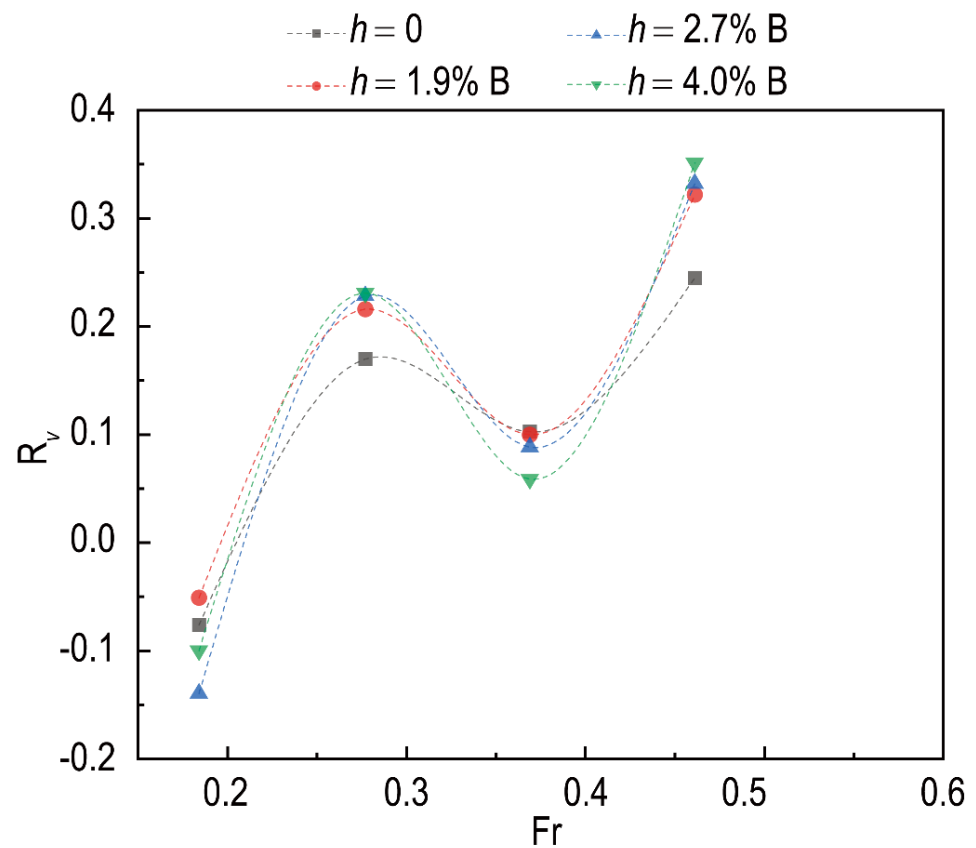


Figure 8. Comparison of the effect of velocity ( $\alpha = 180^\circ$ ,  $T = 5.0$  cm).

#### 4.2. Effect of Interceptor

It is found in Figure 7 that the lift coefficient is changed with the velocity in the same tendency in different conditions, but the discrepancy between the results at a certain velocity is different, which means the height of the interceptor is an important factor for the induced lift. Therefore, the relationship between the lift coefficient and the height of the interceptor in the conditions of different velocities is shown in Figure 9.

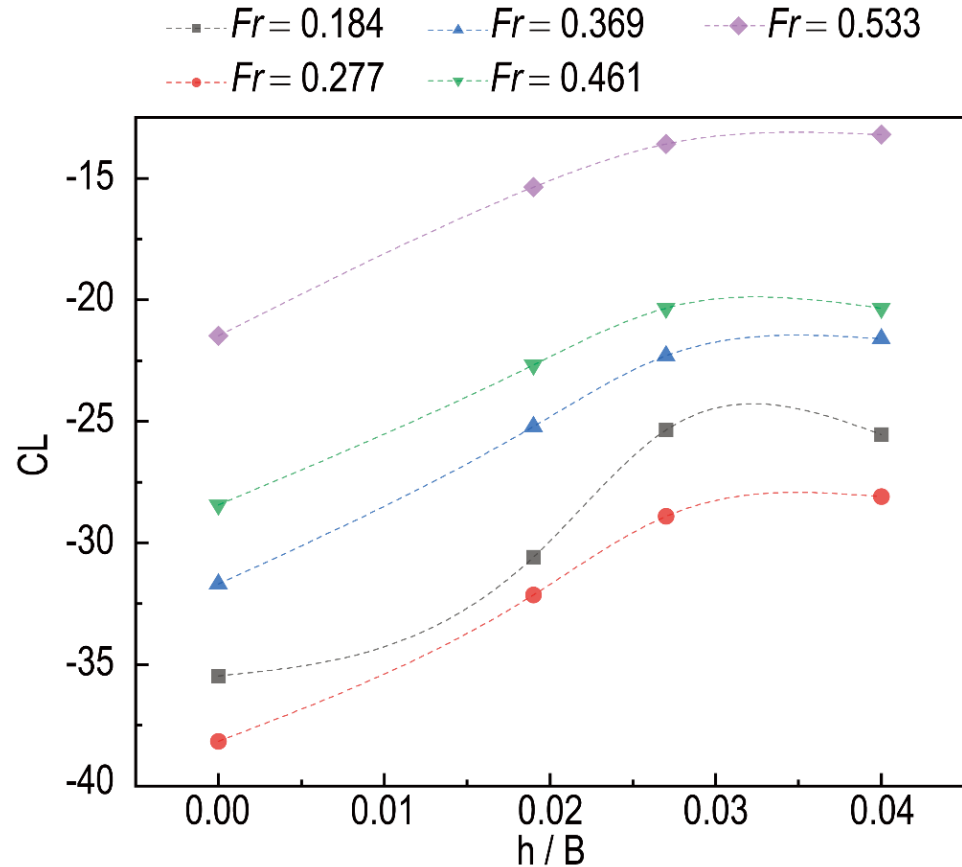


Figure 9. Comparison of the lift coefficients in the conditions of different interceptor heights ( $\alpha = 180^\circ$ ,  $T = 5.0$  cm).

It is demonstrated in Figure 9 that the results in the conditions of different velocities possess the same tendency, and compared with the models without interceptor, the lift coefficient of the model is increased remarkably with the height when the height of the interceptor is not larger than 2.7%  $B$ . The lift coefficient is proportional to the  $h/B$  approximately, which denotes the effect of the interceptor. It is noted that the difference between the lift coefficient of the models with 2.7%  $B$  and 4.0%  $B$  high interceptor can be ignored. It is suggested by the comparison that the effect of the interceptor on lift force has arisen in a limited extent of its height, which is about 2.7%  $B$  (10 mm) in the present condition. Meanwhile, it should be noted that the results in the condition that  $Fr = 0.277$  are less than the others, which denotes the nonlinear influence of speed.

In order to get a better understanding of the effect of the interceptor, a factor  $R_h$  is defined as follow:

$$R_{h(i+1)} = \frac{Cl_{h(i+1)} - Cl_{h(i)}}{|Cl_{h(i)}|} \tag{3}$$

where  $Cl_{h(i)}$  is the lift coefficient in the condition of a certain interceptor,  $Cl_{h(i+1)}$  is the lift coefficient in the condition of a higher interceptor, and the factor  $R_h$  defines the change rate of the lift coefficient caused by the height of the interceptor. The heights of the interceptor

adopted are 1.9%  $B$ , 2.7%  $B$ , and 4.0%  $B$ , and the factors of  $R_h$  in different conditions are compared in Figure 10.

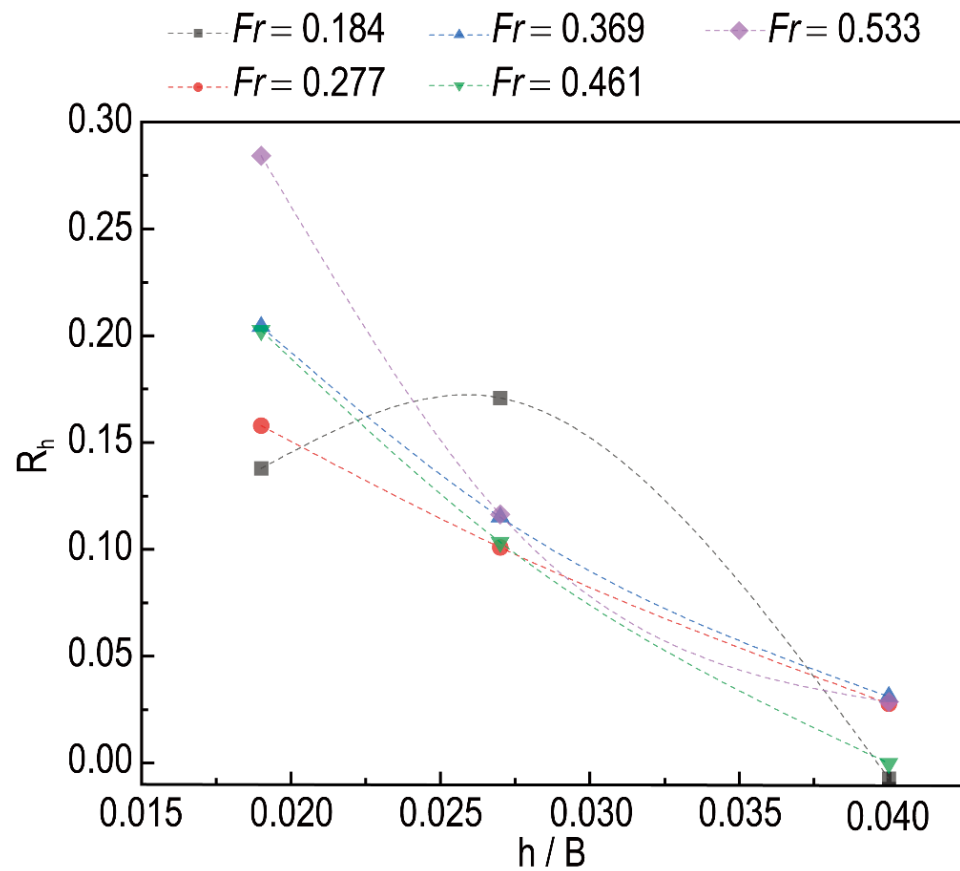


Figure 10. Comparison of the effect of the interceptor ( $\alpha = 180^\circ$ ,  $T = 5.0$  cm).

It is shown in Figure 10 that the change rates of the lift coefficient can be considered into two different types. In the condition that  $Fr = 0.184$ , strong nonlinearity is observed, which means the effect of the interceptor is not remarkable. In the other conditions, curves have a similar tendency and weak nonlinearity, which suggests the influence of the interceptor is enhanced, especially at the condition of  $h < 2.7\% B$ . The value of the last point of each curve is close to 0, which means the lift force is induced by the interceptor. The condition of  $h = 4.0\% B$  has no obvious increase compared to  $h = 2.7\% B$ . This phenomenon is consistent with Figure 9.

It is shown in Figure 8 that there is a nonlinear relationship between the change rate of the lift coefficient and non-dimensional velocity. The lift coefficient is increased with the velocity when the  $Fr > 0.184$ , and the change rates are varied from speed to speed, which means the contribution of velocity is nonlinear. The change rates in the conditions of different interceptors possess the same tendency and little difference, which suggests that the influence of velocity is greater than that of the interceptor. Further, the change rate is affected by the interceptor at each velocity, and the influence is proportional to the height of the interceptor, but there is a limited extent of interceptor height beyond which has little affection. Further discussion will be conducted in Section 4.2.

#### 4.3. Effect of Angle

In the condition that the angle of the plate is decreased, which means the plate is not a flat plate anymore, the flow field around the interceptor will be influenced, and therefore the lift force induced will be changed. Reducing the angle from  $180^\circ$  to  $160^\circ$ , Model 2 is compared to investigate the effect of the angle. The lift coefficients obtained by Equation (1)

in the condition of a 5.0 cm draft are shown in Figure 11. Where  $h$  is the height of the interceptor,  $B$  is the width of the plates. It should be noted that the breadth  $B$  of the three models is the same, and the projected length of the interceptors in the lateral direction of the hull is the same. It is found that the lift coefficients of Model 2 are larger than those of Model 1 in Figure 5 obviously in the same conditions, while the tendency of the results obtained by the two different models is similar. It is indicated that for the plate in the condition of a certain draft, the lift force induced by the interceptor is influenced by the angle of the plates, which is an important factor but is ignored in the previous research. Meanwhile, it should be noted that the lift coefficient of Model 2 is much more susceptible to the interceptor than Model 1 in the condition that  $Fr = 0.184$ . The effect of the interceptor on the lift coefficient is influenced by the angle of the plates, which is not in accordance with Sverre’s study [25] on planing boats.

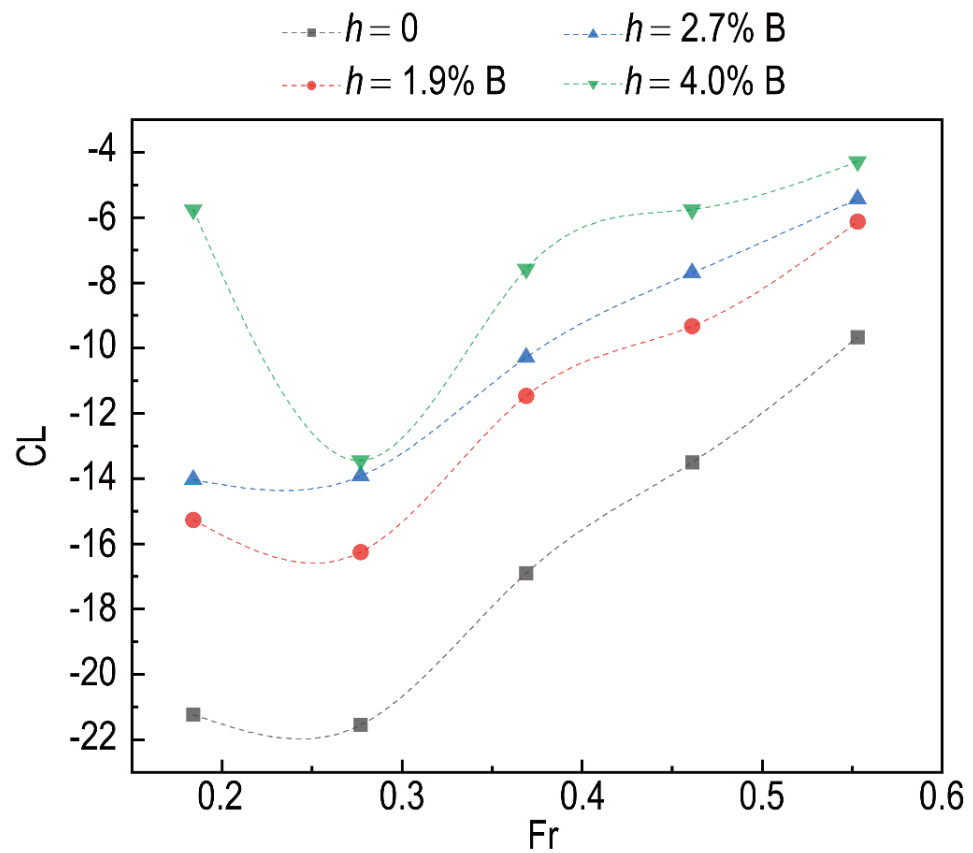


Figure 11. Comparison of the the lift coefficients of Model 2 ( $\alpha = 160^\circ, T = 5.0$  cm).

In order to study the influence caused by the angle, the test data are analyzed in the way as follows:

$$R_\alpha = \frac{\Delta L_{\alpha=160^\circ}}{\Delta L_{\alpha=180^\circ}} = \frac{L_{\alpha=160^\circ, T=5.0\text{cm}} - L_{0, \alpha=160^\circ, T=5.0\text{cm}}}{L_{\alpha=180^\circ, T=5.0\text{cm}} - L_{0, \alpha=180^\circ, T=5.0\text{cm}}} \quad (4)$$

where  $L_{\alpha = 160^\circ, T = 5.0 \text{ cm}}$ , and  $L_{0, \alpha = 160^\circ, T = 5.0 \text{ cm}}$  are the lift force of the plate whose angle  $\alpha$  is  $160^\circ$  with and without interceptor,  $L_{\alpha = 180^\circ, T = 5.0 \text{ cm}}$ , and  $L_{0, \alpha = 180^\circ, T = 5.0 \text{ cm}}$  are the lift force of the plate whose angle  $\alpha$  is  $180^\circ$  with and without interceptor.  $\Delta L_{\alpha = 160^\circ}$  and  $\Delta L_{\alpha = 180^\circ}$  are the lift induced by the interceptor in the conditions that the angle of the model is  $160^\circ$  and  $180^\circ$ , respectively. Therefore, the factor  $R_\alpha$  denotes the influence caused by the angle. The comparison of the results is shown in Figure 12.

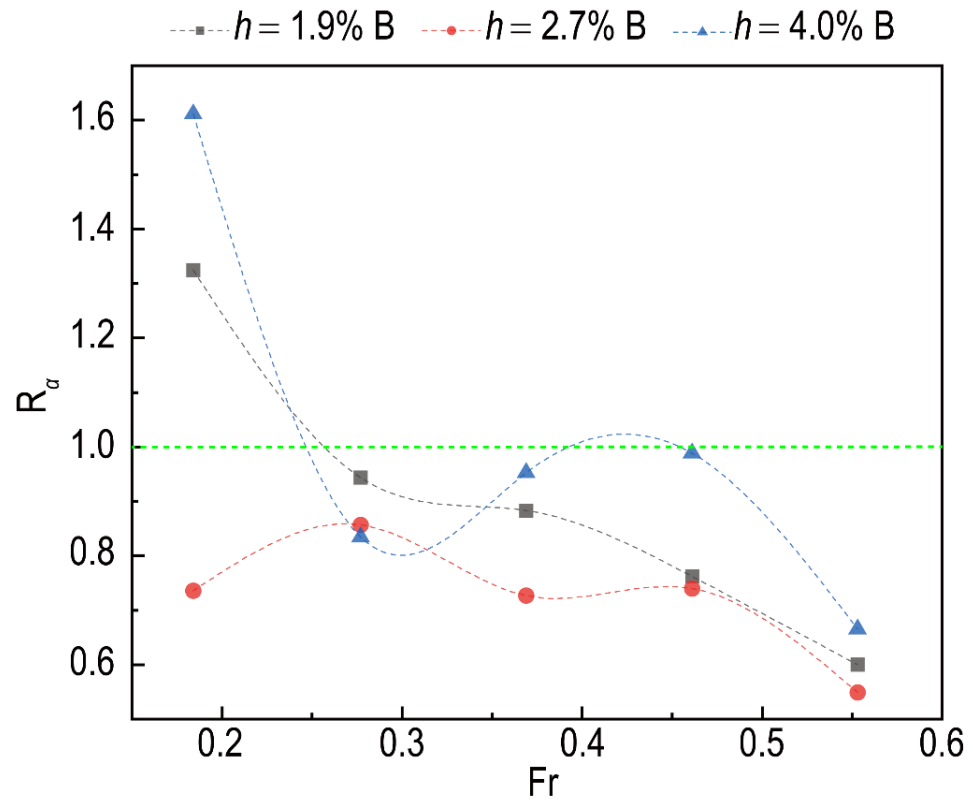


Figure 12. Comparison of the effect of the angle.

It can be found in Figure 12 that the lift induced by the interceptor is decreased with the speed overall. When  $Fr$  is less than 0.277, the results are irregular because of the limited lift force at low velocity. When  $Fr$  is larger than 0.277, the factor  $R_{\alpha}$  is decreased with velocity and less than 1. It is demonstrated that the effect of the interceptor is strongly impacted by the deadrise angle, which is in accordance with the conclusion obtained by Luca et al. [28]

#### 4.4. Effect of Draft

The effect of draft on the lift force induced by the interceptor is rarely studied. Sverre [25] pointed out that the effect of draft and angle on the lift force is negligible for traditional planing boats. In order to validate the effect of draft on the lift force of a submerged plate with angle, the draft of Model 2 is changed from 5.0 cm to 10.0 cm, and the lift force of Model 2 with different interceptors obtained in the corresponding conditions are analyzed as follow:

$$R_T = \frac{\Delta L_{T=10.0\text{cm}}}{\Delta L_{T=5.0\text{cm}}} = \frac{L_{\alpha=160^\circ, T=10.0\text{cm}} - L_{0, \alpha=160^\circ, T=10.0\text{cm}}}{L_{\alpha=160^\circ, T=5.0\text{cm}} - L_{0, \alpha=160^\circ, T=5.0\text{cm}}} \quad (5)$$

where  $L_{\alpha = 160^\circ, T = 10.0 \text{ cm}}$  and  $L_{0, \alpha = 160^\circ, T = 10.0 \text{ cm}}$  are the lift force of the Model 2 with and without interceptor in the condition of 10.0 cm draft,  $L_{\alpha = 160^\circ, T = 5.0 \text{ cm}}$ , and  $L_{0, \alpha = 160^\circ, T = 5.0 \text{ cm}}$  are the lift force of the model with and without interceptor in the condition of 5.0 cm draft.  $\Delta L_{T = 10.0 \text{ cm}}$  and  $\Delta L_{T = 5.0 \text{ cm}}$  are the lift force induced by the interceptor when the draft of the model is 10.0 cm and 5.0 cm, respectively. Therefore, the factor  $R_T$  denotes the influence caused by the draft. The lift coefficients and the comparison of the results in each condition are shown in Figure 13, and the  $Fr$  number adopted is 0.184, 0.277, 0.369, 0.461, and 0.553.

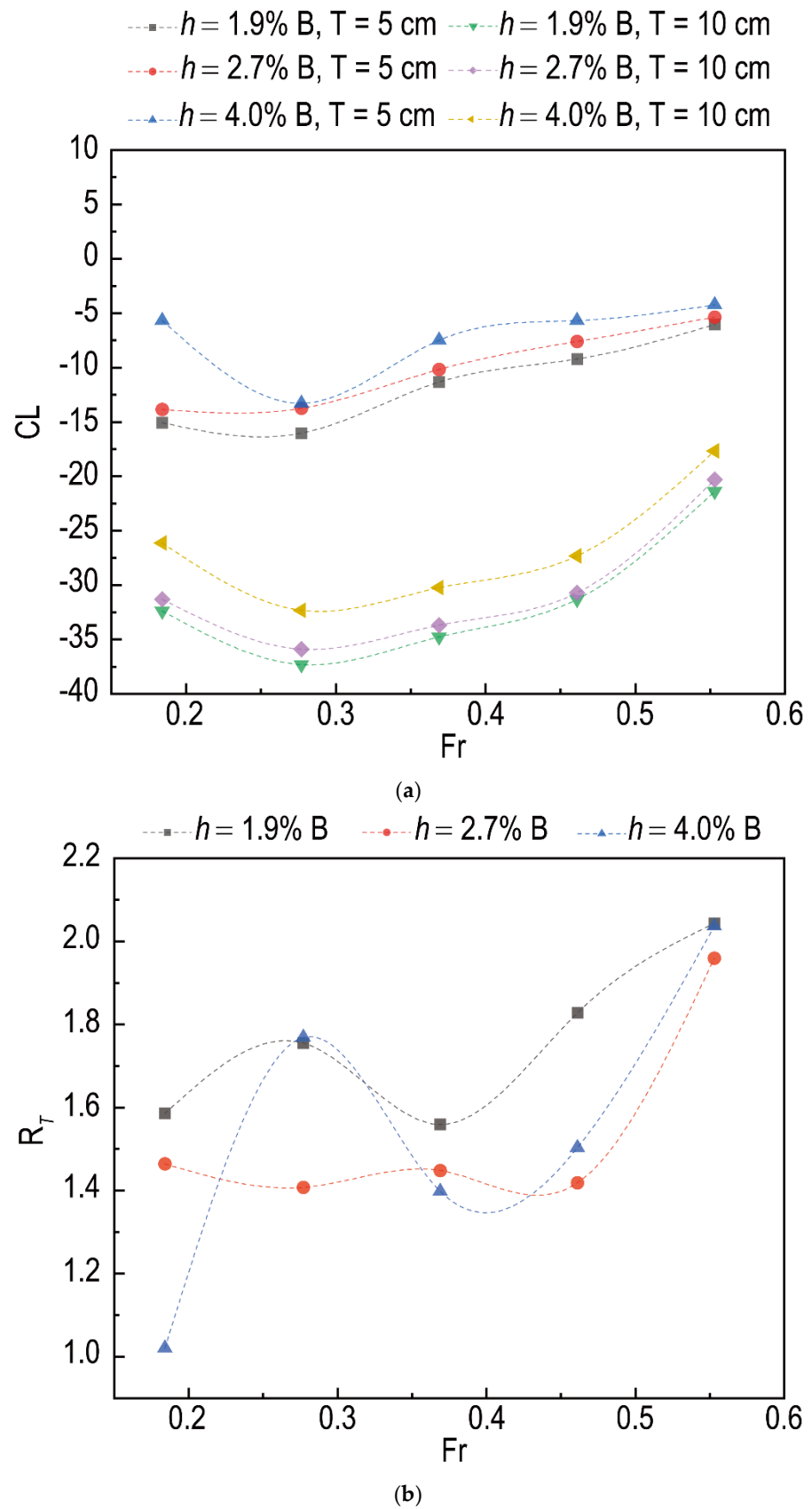


**Figure 13.** Comparison of the effect of the draft. (a) Comparison of the lift coefficients in the conditions of different drafts ( $\alpha = 160^\circ$ ). (b) Comparison of the influence caused by draft.

It is shown in Figure 13a that the lift coefficients in the conditions of different drafts are changed in different ways. In both conditions, the lift coefficients are increased at  $Fr = 0.277$ , obviously from  $Fr = 0.277$  to  $0.369$ , and gradually when  $Fr > 0.369$  in the condition of 5.0 cm draft. In the condition of 10.0 cm draft, the lift coefficient is increased gradually from  $Fr = 0.277$  to  $0.461$  and rapidly when  $Fr > 0.461$ . It is demonstrated in Figure 13a that the lift coefficients in the condition of 10.0 cm draft are less than those in the condition of 5.0 cm, but it should be noted that the reduction of the lift coefficient does not suggest a reduction of the effect caused by the interceptor. The influence of the draft on the effect caused by the interceptor can be found in Figure 13b. Though the results in Figure 13b are irregular, an important conclusion that the factor  $\Delta L_{T=10.0\text{ cm}}/\Delta L_{T=5.0\text{ cm}}$  is larger than 1 can be found directly, which means the effect of the interceptor is enhanced when the draft is increased.

#### 4.5. Coupling Effect of Draft and Angle

It is found in the present research that the effect of the interceptor is weakened when the angle of the plate is decreased and is enhanced in the condition that the draft is increased. An issue regarding the coupling effect arises. In order to investigate the coupling effect of draft and angle, the lift force of the plates with different angles are compared in the conditions of different drafts. The drafts used are 5.0 cm and 10.0 cm, the angles adopted are  $180^\circ$ ,  $160^\circ$ , and  $140^\circ$ . The coupling effect of draft and angle is defined as the factor  $R_{\alpha,T}$ , and the factors in the different conditions are shown as follows.

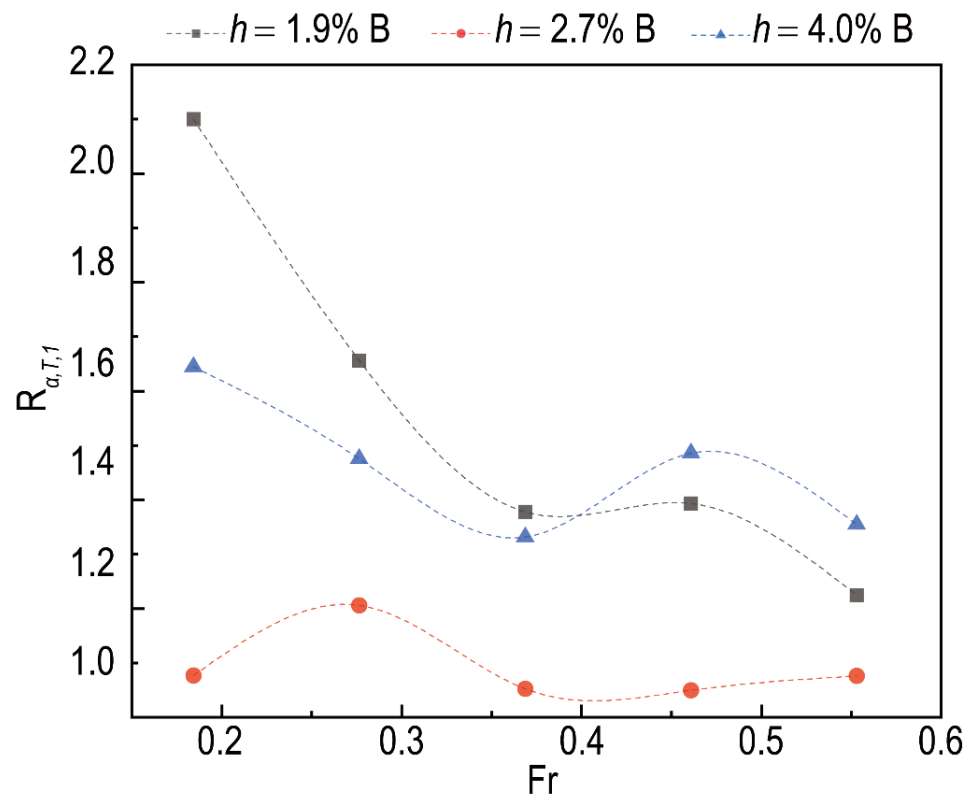
$$R_{\alpha,T,1} = \frac{\Delta L_{\alpha=160^\circ, T=10.0\text{cm}}}{\Delta L_{\alpha=180^\circ, T=5.0\text{cm}}} = \frac{L_{\alpha=160^\circ, T=10.0\text{cm}} - L_{0,\alpha=160^\circ, T=10.0\text{cm}}}{L_{\alpha=180^\circ, T=5.0\text{cm}} - L_{0,\alpha=180^\circ, T=5.0\text{cm}}} \quad (6)$$

$$R_{\alpha,T,2} = \frac{\Delta L_{\alpha=140^\circ, T=10.0\text{cm}}}{\Delta L_{\alpha=160^\circ, T=5.0\text{cm}}} = \frac{L_{\alpha=140^\circ, T=10.0\text{cm}} - L_{0,\alpha=140^\circ, T=10.0\text{cm}}}{L_{\alpha=160^\circ, T=5.0\text{cm}} - L_{0,\alpha=160^\circ, T=5.0\text{cm}}} \quad (7)$$

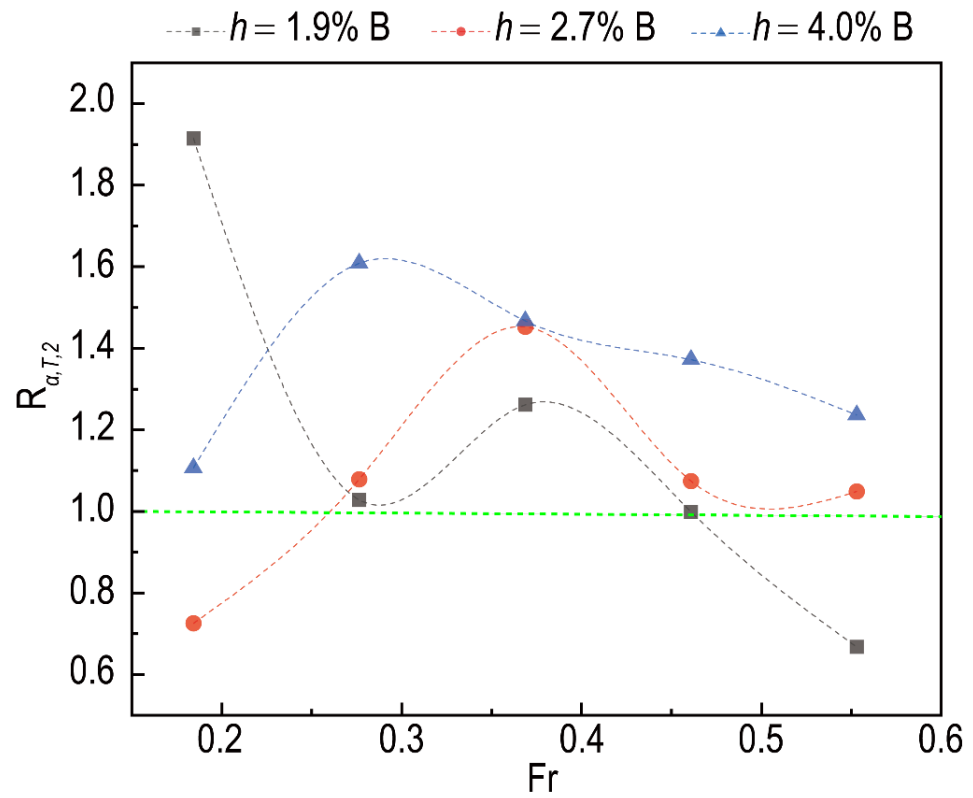
$$R_{\alpha,T,3} = \frac{\Delta L_{\alpha=140^\circ, T=10.0\text{cm}}}{\Delta L_{\alpha=180^\circ, T=5.0\text{cm}}} = \frac{L_{\alpha=140^\circ, T=10.0\text{cm}} - L_{0,\alpha=140^\circ, T=10.0\text{cm}}}{L_{\alpha=180^\circ, T=5.0\text{cm}} - L_{0,\alpha=180^\circ, T=5.0\text{cm}}} \quad (8)$$

where  $L_{\alpha=160^\circ, T=10.0\text{ cm}}$  and  $L_{0,\alpha=160^\circ, T=10.0\text{ cm}}$  are the lift force of the Model 2 with and without interceptor in the condition of 10.0 cm draft.  $L_{\alpha=160^\circ, T=5.0\text{ cm}}$  and  $L_{0,\alpha=160^\circ, T=5.0\text{ cm}}$  are the lift force of the model with and without interceptor in the condition of 5.0 cm draft.  $\Delta L_{T=10.0\text{ cm}}$  and  $\Delta L_{T=5.0\text{ cm}}$  are the lift force induced by the interceptor when the draft of the model is 10.0 cm and 5.0 cm, respectively. Therefore, the factor  $R_T$  denotes the influence caused by the draft. The lift coefficients and the comparison of the results in each condition are shown in Figure 10, and the Fr numbers adopted are 0.184, 0.277, 0.369, 0.461, and 0.553.

Where  $L_{\alpha=160^\circ, T=10.0\text{ cm}}$ ,  $L_{\alpha=180^\circ, T=5.0\text{ cm}}$ ,  $L_{\alpha=140^\circ, T=10.0\text{ cm}}$ , and  $L_{\alpha=160^\circ, T=5.0\text{ cm}}$  are the lift force of the test models with interceptor in the different conditions.  $L_{0,\alpha=160^\circ, T=10.0\text{ cm}}$ ,  $L_{0,\alpha=180^\circ, T=5.0\text{ cm}}$ ,  $L_{0,\alpha=140^\circ, T=10.0\text{ cm}}$ , and  $L_{0,\alpha=160^\circ, T=5.0\text{ cm}}$  are the lift forces of the test models without an interceptor. Therefore,  $\Delta L_{\alpha=160^\circ, T=10.0\text{ cm}}$ ,  $\Delta L_{\alpha=180^\circ, T=5.0\text{ cm}}$ ,  $\Delta L_{\alpha=140^\circ, T=10.0\text{ cm}}$ , and  $\Delta L_{\alpha=160^\circ, T=5.0\text{ cm}}$  are the lift forces induced by the interceptor in the corresponding conditions. The factors  $R_{\alpha,T,1} = \Delta L_{\alpha=160^\circ, T=10.0\text{ cm}}/\Delta L_{\alpha=180^\circ, T=5.0\text{ cm}}$ ,  $R_{\alpha,T,2} = \Delta L_{\alpha=140^\circ, T=10.0\text{ cm}}/\Delta L_{\alpha=160^\circ, T=5.0\text{ cm}}$ , and  $R_{\alpha,T,3} = \Delta L_{\alpha=140^\circ, T=10.0\text{ cm}}/\Delta L_{\alpha=180^\circ, T=5.0\text{ cm}}$  denote the coupling effect of draft and angle in different conditions. The draft is increased by 100% in each comparison, the angle is decreased by about 11.1%, 12.5%, and 22.2%, correspondingly, and the coupling effect is induced by the different variation of angle and consistent variation of the draft. The comparison of the factors in different conditions is shown in Figure 14.



(a)



(b)

Figure 14. Cont.

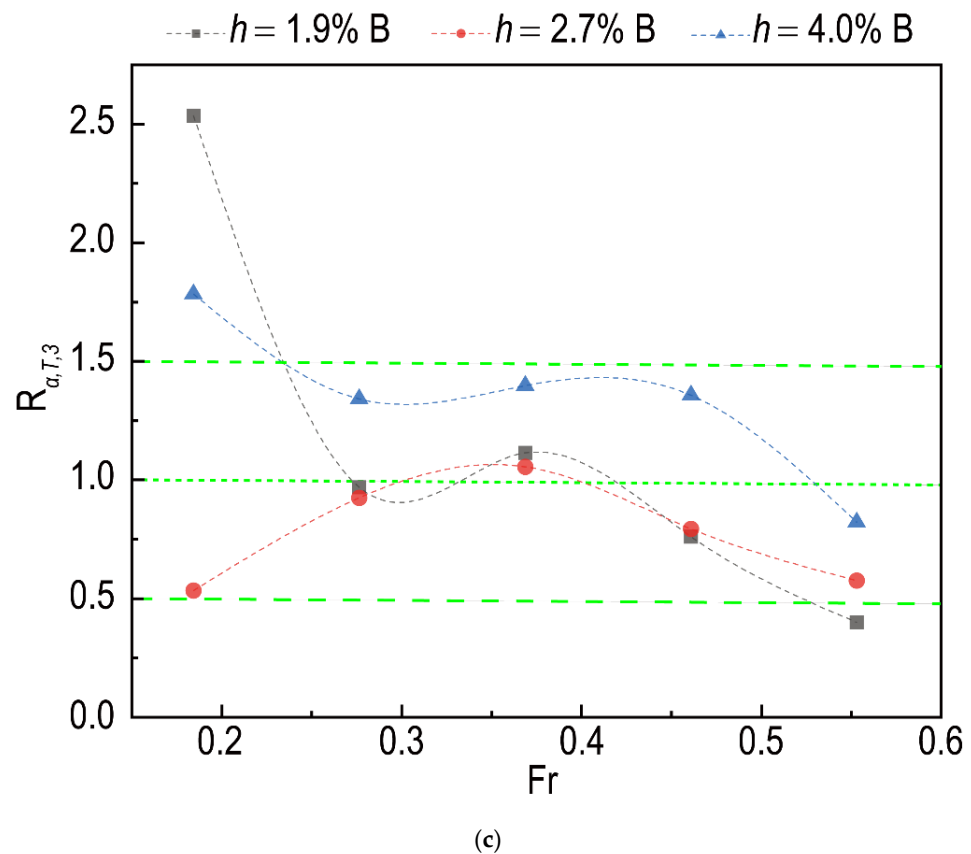


**Figure 14.** Comparison of the coupling effect. (a) Comparison of Model 1 and Model 2 in the conditions of different drafts. (b) Comparison of Model 2 and Model 3 in the conditions of different drafts. (c) Comparison of Model 1 and Model 3 in the conditions of different drafts.

As mentioned previously, the influence of the interceptor is weakened when the angle is decreased and enhanced when the draft is increased. All the results shown in Figure 14a are larger than 1. Compared with the results shown in Figure 12, it is indicated that the influence caused by a 100% increment in the draft is much more effective than an 11.1% reduction in angle. Meanwhile, the factor  $R_{\alpha, T, 1}$  is decreased with the velocity on the whole, which denotes the influence of the angle. Most of the results shown in Figure 14b are larger than 1, which indicates that the influence caused by a 100% increment in the draft is more effective than the one caused by a 12.5% reduction in angle. The influence of the angle can still be observed in the comparison, especially in the conditions that  $Fr > 0.369$  for the plates with 1.9%B and 2.7%B high interceptor and  $Fr > 0.277$  for the plates with 4.0% B high interceptor.

In the condition that the reduction of the angle is 22.2% and increment of the draft is 100%, most of the results shown in Figure 14c are in the extent  $0.5 < R_{\alpha, T, 1} < 1.5$ , which means the influence caused by draft and angle are well-matched. It is demonstrated in Figure 14 that the influence caused by a 100% increment in draft for the present model is equivalent to the one caused by a 22.2% reduction in the angle roughly. Compared with the influence of draft, the effect of angle seems greater. The lift force of the model with a 4.0% B height interceptor is not sensitive to deadrise angle, the lift force of the model with a 2.7% B height interceptor is not sensitive to draft and the coupled effect. That is the reason why the trendline of the  $h = 2.7\% B$  is slightly different from the other cases. However, it is difficult to understand why the induced lift force is not sensitive to some of the factors and the coupled effect by the model test. CFD investigation is still necessary.

## 5. Conclusions

In this study, the effects of velocity and interceptor height on the lift force of the plate with different angles, as well as the influence of angle and draft on this effect, are investigated. The conclusions obtained are as follows:

- (a) Velocity is the key factor dominating the effect of the interceptor. The lift coefficient of the test model with the interceptor in the present investigation is proportional to the square of  $Fr$ , but the contribution of velocity to the lift coefficient of the plate with the interceptor is changed from speed to speed;
- (b) The height of the interceptor is an important factor. The lift coefficient is approximately proportional to the square of  $h/B$  at high speeds, but the effect of the interceptor exits in a limited extent of its height, which is about 2.7%  $B$  (10 mm) for the present model;
- (c) The influence of angle and draft on the effect of the interceptor cannot be neglected for the present study. The effect of the interceptor is weakened when the angle of the plate is reduced and is enhanced when the draft is increased. The influence caused by a 100% increment in the draft for the present model is roughly equivalent to the one caused by a 22.2% reduction in the angle, and compared with the influence of the draft, the effect of angle seems greater.

The six degrees of freedom of the test model adopted in the present study is constrained. It is useful to investigate the lift force induced and the affecting factors, but it is not suitable for the investigation of the other performance, such as the heave and trim motion and resistance of the model. Further study on the details of the flow field and the formula of the lift force caused by the interceptor is still necessary.

**Author Contributions:** Conceptualization, R.D. and T.W.; methodology, Z.Z.; software, F.L.; validation, R.D., P.S. and T.W.; formal analysis, Z.Z.; investigation, Z.Z.; resources, T.W.; data curation, T.W.; writing—original draft preparation, R.D. and T.W.; writing—review and editing, Z.Z. and T.W.; visualization, R.D., Z.Z., F.L. and T.W.; supervision, R.D. and T.W.; project administration, R.D. and T.W.; funding acquisition, R.D., P.S. and T.W. All authors have read and agreed to the published version of the manuscript.

**Funding:** Financial support was provided by the Project of Research and Development Plan in Key Areas of Guangdong Province (grant no. 2020B1111010002); the National Key Research and Development Program of China (No. 2021YFC2800700); the National Natural Science Foundation of China (grant no. 52171330; 52101379; 52101380; 51679053); the Guangdong Basic and Applied Basic Research Foundation (2019A1515110721); the China Postdoctoral Science Foundation (grant no. 2019M663243) and the Natural Science Foundation of Guangdong Province, China (2021A1515012134). The APC was funded by the Project of Research and Development Plan in Key Areas of Guangdong Province (grant no. 2020B1111010002).

**Institutional Review Board Statement:** Not applicable.

**Informed Consent Statement:** Not applicable.

**Data Availability Statement:** The data that support the findings of this study are available within the article.

**Conflicts of Interest:** The authors declare no conflict of interest.

## References

1. Zselezky, J.; Hays, J. *FFG-7 Model Powing Test With and Without a Stern Wedge*; US Naval Academy Report EW-28-84; Hydromechanics Laboratory: Annapolis, MD, USA, 1984.
2. Zselezky, J.; Johnson, B. *Effects of a Bow Bulb and Various Stern Wedge on the EHP of FFG-7 Class Frigates*; US Naval Academy Report EW-6-84; Hydromechanics Laboratory: Annapolis, MD, USA, 1984.
3. Karimi, M.H.; Seif, M.S.; Abbaspour, M. An experimental study of interceptor's effectiveness on hydrodynamic performance of high-speed planing crafts. *Pol. Marit. Res.* **2013**, *20*, 21–29. [[CrossRef](#)]
4. Karimi, M.H.; Seif, M.S.; Abbaspour, M. A study on vertical motions of high-speed planing boats with automatically controlled stern interceptors in calm water and head waves. *Ships Offshore Struct.* **2015**, *10*, 335–348. [[CrossRef](#)]

5. Park, J.-Y.; Choi, H.; Lee, J.; Choi, H.; Woo, J.; Kim, S.; Kim, D.J.; Kim, S.Y.; Kim, N. An experimental study on vertical motion control of a high-speed planing vessel using a controllable interceptor in waves. *Ocean Eng.* **2019**, *173*, 841–850. [[CrossRef](#)]
6. Mansoori, M.; Fernandes, A.C. The interceptor hydrodynamic analysis for controlling the porpoising instability in high speed crafts. *Appl. Ocean Res.* **2016**, *57*, 40–51. [[CrossRef](#)]
7. Talaat, W.M.; Hafez, K.A.; Banawan, A.A. A CFD presentation and visualization for a new model that uses interceptors to harness hydro-energy at the wash of fast boats. *Ocean Eng.* **2017**, *130*, 542–556. [[CrossRef](#)]
8. Ghassemi, H.; Mansouri, M.; Zaferanlouei, S. Interceptor hydrodynamic analysis for handling trim control problems in the high-speed crafts. *Proc. Inst. Mech. Eng.* **2011**, *225*, 2597–2618. [[CrossRef](#)]
9. Mansoori, M.; Fernandes, A.C. Interceptor and trim tab combination to prevent interceptor's unfit effects. *Ocean Eng.* **2017**, *134*, 140–156. [[CrossRef](#)]
10. Mansoori, M.; Fernandes, A.C. Hydrodynamics of the Interceptor Analysis Via Both Ultrareduced Model Test and Dynamic Computational Fluid Dynamics Simulation. *J. Offshore Mech. Arct. Eng.* **2017**, *139*, 021101. [[CrossRef](#)]
11. Mansoori, M.; Fernandes, A.C.; Ghassemi, H. Interceptor design for optimum trim control and minimum resistance of planing boats. *Appl. Ocean Res.* **2017**, *69*, 100–115. [[CrossRef](#)]
12. Guo, C.Y.; Song, K.W.; Gong, J.; Jing, T. Influence of interceptor on deep-V ship's resistance performance. *J. Harbin Eng. Univ.* **2018**, *39*, 215–221.
13. Zhu, F.; Chen, J.W.; He, S.L.; Ni, Q.J. Study on drag reduction mechanism of high speed deep-V boat with interceptor. *Wuhan Ligong Daxue Xuebao/J. Wuhan Tec. Univ.* **2019**, *43*, 1007–1011.
14. Song, K.W.; Guo, C.Y.; Gong, J.; Li, P.; Wang, W. Numerical study on the effect of interceptor on the resistance and wake field of twin-screw ship. *J. Shanghai Jiaotong Univ.* **2019**, *53*, 957–964. [[CrossRef](#)]
15. Shen, Y.L.; Gao, X.P.; Huo, C. Influence of interceptor on resistance performance of planning boat. *Ship Sci. Technol.* **2020**, *42*, 30–33.
16. Seok, W.; Park, S.Y.; Rhee, S.H. An experimental study on the stern bottom pressure distribution of a high-speed planing vessel with and without interceptors. *Int. J. Nav. Arch. Ocean Eng.* **2020**, *12*, 691–698. [[CrossRef](#)]
17. Pacuraru, F.; Presura, A.; Pacuraru, S. Experimental towing tank tests on high speed displacement ship. In Proceedings of the IOP Conference Series: Materials Science and Engineering, Iasi, Romania, 23–27 June 2020; Volume 916, p. 012080.
18. Jacobi, G.; Thill, C.H.; Veer, R.V.; Huijsmans, R.H.R. Analysis of the influence of an interceptor on the transom flow of a fast ship by pressure reconstruction from stereoscopic scanning PIV. *Ocean Eng.* **2019**, *181*, 281–292. [[CrossRef](#)]
19. Song, K.-W.; Guo, C.-Y.; Wang, C.; Gong, J.; Li, P. Investigation of the influence of an interceptor on the inlet velocity distribution of a waterjet-propelled ship using SPIV technology and RANS simulation. *Ships Offshore Struct.* **2019**, *15*, 138–152. [[CrossRef](#)]
20. Suneela, J.; Krishnankutty, P.; Anantha Subramanian, V.A. Numerical investigation on the hydrodynamic performance of high-speed planing hull with transom interceptor. *Ships Offshore Struct.* **2021**, *15*, S134–S142. [[CrossRef](#)]
21. Luca, F.; Pensa, C. The prediction of the interceptor performances based on towing tank test data Ship-model correlation and hull form influence. In Proceedings of the IMAM 2013, 15th International Congress of the International Maritime Association of the Mediterranean (IMAM), Coruña, Spain, 14–17 October 2013.
22. Sverre, S. Experimental investigation of interceptor performance. In Proceedings of the 9th International Conference on Fast Sea Transportation FAST2007, Shanghai, China, 23–27 September 2007.
23. Srikanth, S.; Raju, D. Performance Prediction of High-Speed Planing Craft With Interceptors Using a Variation of the Savitsky Method. In Proceedings of the First Chesapeake Power Boat Symposium, Annapolis, MD, USA, 7–8 March 2008; Society of Naval Architects and Marine Engineers: Alexandria, VA, USA, 2008.
24. Savitsky, D. Hydrodynamic Design of Planing Hulls. *Mar. Technol. SNAME News* **1964**, *1*, 71–95. [[CrossRef](#)]
25. Luca, F.; Pensa, C.; Pranzitelli, A. Experimental and numerical investigation on interceptors' effectiveness. In Proceedings of the 7th Conference on High Performance Marine Vehicles, Melbourne, FL, USA, 13–15 October 2010.
26. Mansoori, M.; Fernandes, A.C. Hydrodynamics of the interceptor on a 2-D flat plate by CFD and experiments. *J. Hydrodyn.* **2015**, *27*, 919–933. [[CrossRef](#)]
27. Zhou, G.L. Uncertainty Analysis of Ship Model Resistance Test in Towing Tank. Harbin Engineering University. 2002. Available online: <http://dx.chinadoi.cn/10.7666/d.Y483205> (accessed on 15 January 2022).
28. Deng, R.; Chen, S.Y.; Wu, T.C.; Luo, F.Q.; Jiang, D.P.; Li, Y.L. Investigation on the influence induced by interceptor on the viscous flow field of deep-Vee vessel. *Ocean Eng.* **2019**, *196*, 106735. [[CrossRef](#)]